

CrossMark
click for updatesCite this: *RSC Adv.*, 2015, 5, 15579

Heavier chalcogenone complexes of bismuth(III) trihalides: potential catalysts for acylative cleavage of cyclic ethers†

Katam Srinivas, Paladugu Suresh, Chatla Naga Babu, Arruri Sathyanarayana and Ganesan Prabusankar*

Heavier chalcogenones (S, Se and Te) of imidazole act as versatile ligands to yield a series of mononuclear and dinuclear bismuth(III) complexes of heavier chalcogenones in excellent yield. These new bismuth heavier chalcogen derivatives are the first structurally characterized molecules, where the bismuth and heavier chalcogen ratio is 1 : 1. There is only one previous report of a crystal structure of a bismuth(III)–imidazol selone compound and none with bismuth(III)–imidazol tellone. The bismuth center in monomeric bismuth chalcogen trihalides depicts pseudo trigonal bipyramidal geometry, while the dimeric bismuth chalcogen trihalides demonstrate distorted square pyramidal geometry. The solid state structures of bismuth chalcogenone derivatives feature rare Bi⋯π(aryl) interactions. Thus, the centroid of the C6-ring suggests a half sandwich type of bismuth environment in mononuclear and dinuclear bismuth(III) chalcogenone complexes. Notably, the Bi⋯π(aryl) interaction is not often noticed for mononuclear bismuth chalcogen compounds. Some of the bismuth(III) chalcogenone complexes also exhibit C–H⋯π(aryl), C–H⋯S and C–H⋯Cl types of hydrogen bonding. The bismuth–chalcogen bond distance in mononuclear bismuth(III)tribromide chalcogenone complexes is slightly longer than in mononuclear bismuth(III)trichloride chalcogenone complexes. A gradual increase in carbon–chalcogen bond distance was observed from the free imidazole–chalcogenone to mononuclear bismuth(III)–trichloride chalcogenones, dinuclear bismuth(III)trichloride chalcogenones and mononuclear bismuth(III)–tribromide chalcogenones and dinuclear bismuth(III)tribromide chalcogenones. The UV-vis absorption properties and thermal decomposition properties of imidazol chalcogenones and their bismuth derivatives were investigated. Furthermore, the *O*-acylative cleavage of cyclic ethers was demonstrated using mononuclear and dinuclear bismuth(III) complexes of heavier chalcogenones as catalysts. In contrast to bismuth(III)trichloride and bismuth(III)tribromide catalysts, mononuclear and dinuclear bismuth(III) complexes of heavier chalcogenones are very active towards an acylative cleavage of cyclic ethers through a mild and regioselective strategy. In particular, mononuclear imidazolthione–bismuth(III)–trichloride is very active towards *O*-acylative cleavage of 2-methyl tetrahydrofuran.

Received 27th December 2014

Accepted 22nd January 2015

DOI: 10.1039/c4ra17144f

www.rsc.org/advances

Introduction

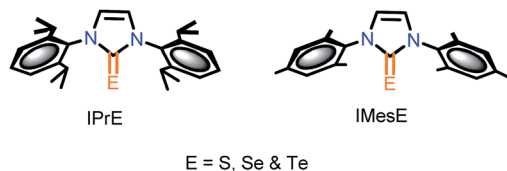
The chemistry of multidentate ligands with “soft” Lewis donors such as chalcogens has attracted much attention in the area of supramolecular,¹ medicinal² and materials chemistry.^{3–6} In particular, a family of compounds bearing imidazole chalcogenone ligands with metals have been probed for studies in fundamental coordination chemistry to understand their ability

to form diverse coordination network architectures in biological systems.² The applications and coordination chemistry of thiones and selones with transition metals has been widely surveyed by Mitzel,^{7a–b} Spicer,^{7c} Raper,^{8,9} Parkin,¹⁰ Pettinari,¹¹ and Akrivos *et al.*;¹² whereas there are very few examples of the coordination chemistry of main group metal–thiones, selones and tellones known in the literature. Especially, the heavy main group p-block atoms have a known propensity to form supramolecular or polynuclear aggregates with or without metal⋯metal interactions.¹³

In particular, (Scheme S1, see ESI†) the heavier p-block element bismuth forms monomeric, dimeric and tetrameric complexes of imidazole–chalcogenones with different imidazole chalcogenone ligands.^{14–23} The monomeric bismuth imidazole chalcogenone complexes, [LBi(NO₃)₂], L = hydro-[tris(3-phenyl-2-thioimidazolyl)]borate,¹⁵ [Bi(Tt)₂Cl], Tt =

Department of Chemistry, Indian Institute of Technology Hyderabad, ODF Campus, Yeddumailaram, Telangana, India-502 205. E-mail: prabu@iith.ac.in; Fax: +91 40 2301 6032; Tel: +91 40 2301 6089

† Electronic supplementary information (ESI) available: Scheme S1, FT-IR, NMR and UV-vis for 3–17. CCDC 1000479–1000484 and 1011929–1011933. For ESI and crystallographic data in CIF or other electronic format see DOI: 10.1039/c4ra17144f



Scheme 1 IPrE and IMesE ligands used in the present work.^{26–28}

hydrottris(thioxotriazolyl)-borate,¹⁶ $[\{\text{Bi}(\text{Tr}^{\text{Ph,Me}})_2\}_2\text{NO}_3]$, $\text{Tr}^{\text{Ph,Me}} =$ hydrotris(1,4-dihydro-3-methyl-4-phenyl-5-thioxo-1,2,4-triazolyl)-borato,¹⁷ $[\{\text{Bi}(\text{Tr}^{\text{Et,Me}})_2\}_2\text{NO}_3]$, $\text{Tr}^{\text{Et,Me}} =$ hydrotris(1,4-dihydro-3-methyl-4-ethyl-5-thioxo-1,2,4-triazolyl)borato,¹⁸ and $[(\text{Tm}_2\text{Bi})-(\text{Tp}_2\text{Na})]$, $\text{Tm} =$ hydrotris(methimidazolyl)borate, $\text{Tp} =$ hydrotris-(pyrazolyl)borate¹⁹ were derived from tripodal S_3 ligands of the tris(mercaptoimidazolyl)borate type ligands. The only monomeric bismuth imidazole chalcogenone complex known with bidendate ligand is $[\{\text{CH}_2(\text{HCN}_2\text{Me})_2\text{C}(\text{S})\}\text{BiCl}_3]$.²⁰ The dimeric bismuth imidazole chalcogenone complexes, $[(\text{BiCl}_3(\text{mipimdt})_2)_2]$, $\text{mipimdt} = N$ -methyl- N' -isopropyl-imidazolidine-2-thione, $[(\text{BiCl}_3(\text{mpimdt})_2)_2]$, $\text{mpimdt} = N$ -methyl- N' -propylimidazolidine-2-thione²¹ and $[(\text{BiCl}_3(\text{deimdt})_2)_2]$, $\text{deimdt} = NN'$ -diethylimidazolidine-2-thione²² were isolated from monodendate N,N' -substituted imidazolidine-2-thiones. Notable exception was $[(\text{Tm})\text{BiCl}(\mu\text{-Cl})_2]$ obtained from tridendate hydrotris(methimidazolyl)borate.¹⁹ Recently, Singh *et al.* reported the first tetranuclear bismuth selone compound, $[\{(\text{nbimds})\text{Bi}\}_4]$, $\text{nbimds} = N,N'$ - n -butylimidazolidine-2-selone with bismuth : selone ratio of 1 : 1.²³

The bismuth centers in known bismuth imidazole chalcogenone complexes are hexa-coordinated with octahedral or distorted octahedral geometry, where the bismuth : chalcogen ratio is [1 : 1], [1 : 2], [1 : 3] or [1 : 6]. Notably, (i) the systematic design and exploration of thione, selone and tellone-containing imidazole ligands towards bismuth salts, (ii) bismuth imidazole chalcogenone complexes with less than six coordination number and (iii) monomeric or dimeric bismuth imidazole chalcogenone complexes with bismuth : chalcogen ratio of 1 : 1 are not known. This work describes the synthesis of monomeric or dimeric bismuth imidazole chalcogenone complexes with IPrE and IMesE ligands, with the aim of answering points (i)–(iii) (*vide supra*) (Scheme 1).^{26–28} In addition, applications of these complexes to the *O*-acylative cleavage of various cyclic ethers are explored.

Experimental

Materials and methods

All manipulations were carried out under an argon atmosphere in a glove box. The solvents were purchased from commercial sources and purified according to standard procedures.³⁹ Unless otherwise stated, the chemicals were purchased from commercial sources. IPrHCl (**1**), IPrHPF_6 (**2**),⁴⁰ $\text{IPr}=\text{S}$ (**3**) and $\text{IPr}=\text{Se}$ (**4**),²⁶ IMesHCl (**1a**), $\text{IMes}=\text{S}$ (**3a**),²⁷ $\text{IMes}=\text{Te}$ (**5a**)²⁸ were prepared as previously reported. BiCl_3 (product code: 224839, $\geq 98\%$) and BiBr_3 (product code: 401072, $\geq 98\%$) were purchased from Sigma Aldrich and used as received. FT-IR measurement (neat) was carried out on a Bruker Alpha-P

Fourier transform spectrometer. NMR spectra were recorded on Bruker Ultrashield-400 spectrometers at 25 °C unless otherwise stated. Chemical shifts are given relative to TMS and were referenced to the solvent resonances as internal standards. Thermogravimetric analysis (TGA) was performed using a TA-SDT Q600, Tzero-press. The UV-vis spectra were measured on a T90+ UV-visible spectrophotometer. Elemental analyses were performed by the Euro EA-300 elemental analyzer. The crystal structures of **3**, **5**, **4a**, **6–9** and **12–15** were measured on an Oxford Xcalibur 2 diffractometer. Single crystals of **3** suitable for the single crystal X-ray analysis were obtained from its saturated solution in dichloromethane, layered with *n*-hexane at room temperature, while **5** was obtained from a mixture of *n*-hexane and toluene at room temperature. Single crystals of **6** and **7** suitable for the X-ray analysis were obtained from their saturated solutions in chloroform, layered with *n*-hexane at room temperature, while **8** and **9** were obtained from their saturated solutions in dichloromethane, layered with *n*-hexane at room temperature. Single crystals of **12** and **13** suitable for the X-ray analysis were obtained from their saturated solutions in chloroform, layered with *n*-hexane at room temperature, while **14** and **15** were obtained from their saturated solutions of dichloromethane, layered with *n*-hexane at room temperature. Suitable single crystals for X-ray structural analysis of ligands, **3**, **5**, **4a**, **6–9** and **12–15** were mounted at low temperature (150 K) in inert oil under liquid nitrogen atmosphere. The crystal was kept at 150 K during data collection. Using Olex2,⁴¹ the structure was solved with the ShelXS⁴² structure solution program using Direct Methods and refined with the olex2.refine refinement package using Gauss–Newton minimization. In **9** and **14**, an elevated value for the largest parameter shift per s.u. is observed due to disordered lattice solvent molecule. The appropriate restraints did not help to stabilize ill-defined and oscillating parameters.†

Synthesis of $\text{IPr}=\text{Te}$ (**5**)

Method-I. A mixture of $\text{IPr}\cdot\text{HPF}_6$ (0.555 g, 1.03 mmol), Te (0.158 g, 1.24 mmol) and K_2CO_3 (0.172 g, 1.24 mmol) in methanol (50 mL) was heated at reflux for 4 days, after which the methanol was removed. The remaining solid was taken up in CH_2Cl_2 (2×30 mL), then the solution was filtered and the solvent was evaporated. The compound **5** was crystallized from toluene and hexane mixture. Yield: 70% (based on **2**).

Method-II. Te powder (0.555 g, 4.35 mmol) and potassium *tert*-butoxide (0.488 g, 4.35 mmol) were added to a solution containing $\text{IPr}\cdot\text{HCl}$ (1.541 g, 3.62 mmol) in THF (40 mL) under nitrogen atmosphere. The reaction mixture was stirred for 48 h at room temperature, quenched in water (50 mL), extracted with dichloromethane, dried over sodium sulfate and evaporated. The residue was dissolved in toluene (5 mL) and petroleum ether (15 mL) to separate the impurity from solution. The solution was filtered, evaporated and the residue was dissolved in diethylether and petroleum ether (3 : 1) to afford **5**. Yield: 75% (based on **1**). M.p.: 151–153 °C (dec.). Elemental analysis calcd (%) for $\text{C}_{27}\text{H}_{36}\text{N}_2\text{Te}$ (516.20): C, 62.82; H, 7.03; N, 5.43; found: C, 63.0; H, 6.9; N, 5.3. ¹H NMR (400 MHz, CDCl_3): $\delta =$

7.45–7.41 (t, 2H, CH_{para}), 7.25–7.23 (d, 4H, CH_{meta}), 7.18 (s, 2H, ImH), 2.56–2.46 (sept, 4H, 1PrCH), 1.31–1.29, 1.11–1.10 (d, 24H, CH_3) ppm. ^{13}C NMR (100 MHz, $CDCl_3$): δ = 145.89 (C=Te), 137.87, 135.53, 130.45, 124.36, 123.48 (ArC), 29.25 (1PrCH), 24.63, 23.41 (CH_3) ppm. FT-IR (neat): ν = 3050(m), 2958(s), 2865(m), 1593(m), 1555(m), 1465(s), 1407(m), 1325(s), 1272(m), 1209(m), 1182(vw), 1163(vw), 1107(m), 1060(m), 937(s), 800(s), 738(s) cm^{-1} .

Synthesis of IMes=Se (4a)

A mixture of IMes·HCl (1.5 g, 3.52 mmol), Se (0.278 g, 3.52 mmol) and K_2CO_3 (0.585 g, 4.23 mmol) in methanol (50 mL) was heated at reflux for 24 h after which the methanol was removed. The remaining solid was taken up in CH_2Cl_2 (2 × 30 mL), then the solution was filtered and the solvent was evaporated. **4a** was crystallized from CH_2Cl_2 and hexane mixture. Yield: 68% (based on IMes·HCl). M.p.: 219–220 °C (dec.). Elemental analysis calcd (%) for $C_{21}H_{24}N_2Se$ (383.40): C, 65.79; H, 6.31; N, 7.31; found: C, 65.8; H, 6.3; N, 7.3. 1H NMR (400 MHz, $CDCl_3$): δ = 7.00 (s, 4H, CH_{meta}), 6.95 (s, 2H, ImH), 2.33 (s, 6H, CH_{3para}), 2.11 (s, 12H, CH_{3ortho}) ppm. ^{13}C NMR (100 MHz, $CDCl_3$): δ = 157.49(C=Se), 139.43, 135.42, 134.42, 129.33, 120.26 (ArC), 21.25 ($p-CH_3$), 18.08 ($o-CH_3$) ppm. FT-IR (neat): ν = 2915(w), 1607(w), 1554(w), 1484(m), 1405(m), 1340(s), 1229(m), 1164(w), 1123(m), 1084(s), 925(m), 853(s), 720(s) cm^{-1} .

Synthesis of [(IPr=S)BiCl₃]·CHCl₃ (6)

A solution of **3** (0.056 g, 0.134 mmol) and $BiCl_3$ (0.042 g, 0.134 mmol) in toluene (3 mL) was stirred for 24 h under inert atmosphere at 100 °C, resulting in the formation of light yellow solution. The light yellow crystals of **6** were obtained from its saturated solutions of chloroform, layered with *n*-hexane at room temperature. Yield: 85% (based on $BiCl_3$). M.p.: 257–259 °C (dec.). Elemental analysis calcd (%) for $C_{28}H_{37}BiCl_6N_2S$ (855.38): C, 39.32; H, 4.36; N, 3.28; found: C, 39.2; H, 4.3; N, 3.2. 1H NMR (400 MHz, $CDCl_3$): δ = 7.51–7.47 (t, 2H, ArH), 7.33–7.31 (d, 4H, ArH), 7.02 (s, 2H, ImH), 2.76–2.65 (sept, 4H, 1PrCH), 1.37–1.35, 1.23–1.21 (d, 24H, CH_3) ppm. ^{13}C NMR (100 MHz, $CDCl_3$): δ = 162.14 (C=S), 146.15 (ImC), 134.43, 130.22, 124.26, 121.11 (ArC), 29.04 (1PrCH), 24.37, 23.41 (CH_3) ppm. FT-IR (neat): ν = 2958(m), 2921(s), 2853(m), 1580(w), 1557(w), 1460(s), 1419(m), 1368(s), 1257(m), 1212(m), 1181(m), 1124(m), 1058(m), 936(s), 803(s), 750(s) cm^{-1} .

Synthesis of [(IPr=S)BiBr₃]·CHCl₃ (7)

A solution of **3** (0.056 g, 0.134 mmol) and $BiBr_3$ (0.060 g, 0.134 mmol) in toluene (3 mL) was stirred for 24 h under inert atmosphere at 100 °C, resulting in the formation of a clear yellow solution. The yellow crystals of **7** were obtained from its saturated solutions of chloroform, layered with *n*-hexane at room temperature. Yield: 79% (based on $BiBr_3$). M.p.: 263–265 °C (dec.). Elemental analysis calcd (%) for $C_{28}H_{37}BiBr_3Cl_3N_2S$ (988.73): C, 34.01; H, 3.77; N, 2.83; found: C, 33.8; H, 3.6; N, 2.8. 1H NMR (400 MHz, $CDCl_3$): δ = 7.49–7.45 (t, 2H, ArH), 7.31–7.29 (d, 4H, ArH), 7.00 (s, 2H, ImH), 2.73–2.63 (sept, 4H, 1PrCH), 1.34–1.33, 1.20–1.18 (d, 24H, CH_3) ppm. ^{13}C NMR (100 MHz,

$CDCl_3$): δ = 162.08 (C=S), 146.15 (ImC), 134.43, 130.24, 124.27, 121.14 (ArC), 29.05 (1PrCH), 24.38, 23.42 (CH_3) ppm. FT-IR (neat): ν = 2960(s), 2923(m), 2865(m), 1554(w), 1457(s), 1420(m), 1364(s), 1259(m), 1214(m), 1179(m), 1141(m), 1119(m), 1059(m), 935(s), 804(s), 751(m) cm^{-1} .

Synthesis of [(IPr=Se)BiCl₃]·CH₂Cl₂ (8)

A solution of **4** (0.1 g, 0.213 mmol) and $BiCl_3$ (0.067 g, 0.213 mmol) in toluene (3 mL) was stirred for 16 h under inert atmosphere at room temperature, resulting in the formation of yellow precipitate. The yellow precipitate was filtered and dried in vacuum to yield a yellow powder. Single crystals of **8** were grown by slow vapor diffusion of *n*-hexane into dichloromethane solution of **8**. Yield: 93% (based on $BiCl_3$). M.p.: 259–261 °C (dec.). Elemental analysis calcd (%) for $C_{28}H_{38}BiCl_5N_2Se$ (867.83): C, 38.75; H, 4.41; N, 3.23; found: C, 38.7; H, 4.3; N, 3.2. 1H NMR (400 MHz, $CDCl_3$): δ = 7.69–7.65 (t, 2H, ArH), 7.46–7.44 (d, 4H, ArH), 7.20 (s, 2H, ImH), 5.30 (s, 2H, CH_2Cl_2), 2.63–2.53 (sept, 4H, 1PrCH), 1.36–1.34, 1.23–1.21 (d, 24H, CH_3) ppm. ^{13}C NMR (100 MHz, $CDCl_3$): δ = 159.50 (C=Se), 145.01 (ImC), 133.13, 129.30, 123.25, 120.44 (ArC), 52.46 (2H, CH_2Cl_2), 28.00 (1PrCH), 23.41, 22.35 (CH_3) ppm. FT-IR (neat): ν = 3054(m), 2960(m), 1592(w), 1467(m), 1412(m), 1340(m), 1260(m), 1212(m), 1181(vw), 1095(w), 904(s), 803(m), 727(s) cm^{-1} .

Synthesis of [(IPr=Se)BiBr₃]·CH₂Cl₂ (9)

A Solution of **4** (0.1 g, 0.213 mmol) and $BiBr_3$ (0.095 g, 0.213 mmol) in toluene (3 mL) was stirred for 16 h under inert atmosphere at room temperature, resulting in the formation of reddish brown precipitate. The reddish brown precipitate was filtered and dried *in vacuo* to yield reddish brown powder. Single crystals of **9** were grown by slow vapor diffusion of hexane into dichloromethane solution of **9**. Yield: 89% (based on $BiBr_3$). M.p.: 257–258 °C (dec.). Elemental analysis calcd (%) for $C_{28}H_{37}BiBr_3Cl_2N_2Se$ (1001.18): C, 35.59; H, 3.83; N, 2.80; found: C, 35.6; H, 3.8; N, 2.8. 1H NMR (400 MHz, $CDCl_3$): δ = 7.67–7.64 (t, 2H, ArH), 7.45–7.43 (d, 4H, ArH), 7.04 (s, 2H, ImH), 5.30 (s, 2H, CH_2Cl_2), 2.69–2.59 (sept, 4H, 1PrCH), 1.34–1.33, 1.24–1.22 (d, 24H, CH_3) ppm. ^{13}C NMR (100 MHz, $CDCl_3$): δ = 159.46 (C=Se), 145.04 (ImC), 133.15, 129.31, 123.26, 120.48 (ArC), 52.50 (CH_2Cl_2), 28.00 (1PrCH), 23.40, 22.34 (CH_3) ppm. FT-IR (neat): ν = 2964(m), 1551(w), 1466(m), 1350(m), 1259(m), 1214(w), 1180(w), 1099(w), 903(s), 804(m), 725(s) cm^{-1} .

Synthesis of [(IPr=Te)BiCl₃] (10)

A solution of **5** (0.050 g, 0.0964 mmol) and $BiCl_3$ (0.034 g, 0.0964 mmol) in toluene (3 mL) was stirred for 30 min. under inert atmosphere at 0 °C resulting in the formation of oily brick red precipitate. The oily brick red precipitate was filtered and dried *in vacuo* and washed with hexane (3 × 5 mL) to yield brick red powder. Yield: 94% (based on $BiCl_3$). M.p.: 105–106 °C (dec.). Elemental analysis calcd (%) for $C_{27}H_{36}BiCl_3N_2Te$ (831.52): C, 39.00; H, 4.36; N, 3.37; found: C, 39.0; H, 4.4; N, 3.3. FT-IR (neat): ν = 3050(m), 2961(s), 2867(m), 1591(m), 1547(m), 1462(s), 1409(m), 1327(s), 1260(m), 1209(m), 1182(w), 1102(m), 1060(m), 937(s), 802(s), 754(s) cm^{-1} .

Synthesis of [(IPr=Te)BiBr₃] (11)

A solution of **5** (0.050 g, 0.097 mmol) and BiBr₃ (0.043 g, 0.097 mmol) in toluene (3 mL) was stirred for 30 min. at 0 °C under inert atmosphere, resulting in the formation of reddish brown precipitate. The reddish brown precipitate was filtered and dried *in vacuo* to yield reddish brown powder. Yield: 95% (based on BiBr₃). M.p.: 112–113 °C (dec.). Elemental analysis calcd (%) for C₂₇H₃₆BiBr₃N₂Te (964.88): C, 33.61; H, 3.76; N, 2.90; found: C, 33.6; H, 3.8; N, 2.9. FT-IR (neat): $\nu = 3050(\text{m}), 2961(\text{s}), 2866(\text{m}), 1592(\text{m}), 1548(\text{m}), 1462(\text{s}), 1409(\text{m}), 1326(\text{s}), 1259(\text{m}), 1209(\text{m}), 1182(\text{vw}), 1105(\text{m}), 1060(\text{m}), 937(\text{s}), 801(\text{s}), 753(\text{s}) \text{ cm}^{-1}$.

Synthesis of [(IMesS)Bi(Cl)₂(μ_2 -Cl)]₂·4CHCl₃ (12)

12 was prepared in the same manner as described for **6**. Yield: 84% (Based on BiCl₃). M.p.: 258–260 °C (dec.). Elemental analysis calcd (%) for C₄₆H₅₂Bi₂Cl₁₈N₄S₂ (1781.19): C, 38.69; H, 3.71; N, 4.30; found: C, 38.6; H, 3.7; N, 4.3. ¹H NMR (400 MHz, CDCl₃): $\delta = 7.09$ (s, 8H, CH_{meta}), 6.89 (s, 4H, ImH), 2.37 (s, 12H, CH_{3para}), 2.15 (s, 24H, CH_{3ortho}) ppm. ¹³C NMR (100 MHz, CDCl₃): $\delta = 157.49$ (C=S), 139.42, 135.43, 134.27, 129.33, 120.27 (ArC), 21.26 (*p*-CH₃), 18.08 (*o*-CH₃) ppm. FT-IR (neat): $\nu = 1554(\text{w}), 1482(\text{m}), 1369(\text{s}), 1288(\text{w}), 1239(\text{m}), 1167(\text{vw}), 1138(\text{w}), 1032(\text{w}), 980(\text{w}), 926(\text{w}), 854(\text{s}), 726(\text{s}) \text{ cm}^{-1}$.

Synthesis of [(IMesS)Bi(Br)₂(μ_2 -Br)]₂·4CHCl₃ (13)

13 was prepared in the same manner as described for **7**. Yield: 87% (Based on BiBr₃). M.p.: 265–267 °C (dec.). Elemental analysis calcd (%) for C₄₆H₅₂Bi₂Br₆Cl₁₂N₄S₂ (2047.90): C, 32.12; H, 3.08; N, 3.57; found: C, 32.1; H, 3.0; N, 3.5. ¹H NMR (100 MHz, CDCl₃): $\delta = 7.16$ (s, 8H, CH_{meta}), 6.97 (s, 4H, ImH), 2.42 (s, 12H, CH_{3para}), 2.17 (s, 24H, CH_{3ortho}) ppm. ¹³C NMR (100 MHz, CDCl₃): $\delta = 157.42$ (C=S), 139.41, 135.44, 134.30, 129.35, 120.35 (ArC), 21.30 (*p*-CH₃), 18.12 (*o*-CH₃) ppm. FT-IR (neat): $\nu = 1553(\text{w}), 1483(\text{m}), 1367(\text{s}), 1287(\text{w}), 1236(\text{m}), 1166(\text{vw}), 1138(\text{m}), 1032(\text{w}), 980(\text{m}), 857(\text{s}), 725(\text{m}) \text{ cm}^{-1}$.

Synthesis of [(IMesSe)Bi(Cl)₂(μ_2 -Cl)]₂·4CH₂Cl₂ (14)

Compound **14** was prepared in the same manner as described for **8**. Yield: 85% (Based on BiCl₃). M.p.: 224–226 °C (dec.). Elemental analysis calcd (%) for C₄₆H₅₆Bi₂Cl₁₄N₄Se₂ (1737.20): C, 36.10; H, 3.46; N, 4.01; found: C, 36.0; H, 3.3; N, 4.0. ¹H NMR (400 MHz, CDCl₃): $\delta = 6.92$ (s, 8H, CH_{meta}), 6.88 (s, 4H, ImH), 5.19 (s, 8H, CH₂Cl₂), 2.25 (s, 12H, CH_{3para}), 2.04 (s, 24H, CH_{3ortho}) ppm. ¹³C NMR (100 MHz, CDCl₃): $\delta = 157.49$ (C=Se), 139.42, 135.43, 134.27, 129.33, 120.27 (ArC), 52.15 (CH₂Cl₂), 21.26 (*p*-CH₃), 18.08 (*o*-CH₃) ppm. FT-IR (neat): $\nu = 1550(\text{w}), 1481(\text{m}), 1365(\text{s}), 1234(\text{s}), 1165(\text{w}), 1119(\text{w}), 1034(\text{w}), 927(\text{s}), 855(\text{s}), 738(\text{s}) \text{ cm}^{-1}$.

Synthesis of [(IMesSe)Bi(Br)₂(μ_2 -Br)]₂ (15)

Compound **15** was prepared in the same manner as described for **9**. Yield: 90% (Based on BiBr₃). M.p.: 228–230 °C (dec.). Elemental analysis calcd (%) for C₄₂H₄₈N₄Se₂Bi₂Br₆ (1664.18): C, 30.31; H, 2.91; N, 3.37; found: C, 30.2; H, 2.8; N, 3.3. ¹H NMR (400 MHz, CDCl₃): $\delta = 7.03$ (s, 8H, CH_{meta}), 6.81 (s, 4H, ImH),

2.36 (s, 12H, CH_{3para}), 2.17 (s, 24H, CH_{3ortho}) ppm. ¹³C NMR (100 MHz, CDCl₃): $\delta = 156.69$ (C=Se), 139.48, 135.39, 134.21, 129.36, 120.55 (ArC), 21.28 (*p*-CH₃), 18.12 (*o*-CH₃) ppm. FT-IR (neat): $\nu = 2912(\text{w}), 1561(\text{w}), 1482(\text{m}), 1369(\text{s}), 1231(\text{s}), 1164(\text{w}), 1122(\text{w}), 1033(\text{m}), 927(\text{m}), 858(\text{s}), 721(\text{s}) \text{ cm}^{-1}$.

Synthesis of [(IMesTe)Bi(Cl)₂(μ_2 -Cl)]₂ (16)

Compound **16** was prepared in the same manner as described for **10**. Yield: 65% (based on BiCl₃). M.p.: 108–110 °C (dec.). Elemental analysis calcd (%) for C₄₂H₄₈Bi₂Br₆N₄Te₂ (1494.8): C, 30.31; H, 2.91; N, 3.37; found: C, 30.3; H, 2.9; N, 3.4. FT-IR (neat): $\nu = 1604(\text{m}), 1542(\text{w}), 1481(\text{s}), 1442(\text{w}), 1377(\text{m}), 1320(\text{s}), 1229(\text{s}), 1165(\text{w}), 1107(\text{w}), 1031(\text{s}), 927(\text{m}), 854(\text{s}), 733(\text{s}) \text{ cm}^{-1}$.

Synthesis of [(IMesTe)Bi(Br)₂(μ_2 -Br)]₂ (17)

Compound **17** was prepared in the same manner as described for **11**. Yield: 80% (Based on BiBr₃). M.p.: 120–122 °C (dec.). Elemental analysis calcd (%) for C₄₂H₄₈Bi₂Br₆N₄Te₂ (1761.6): C, 30.31; H, 2.91; N, 3.37; found: C, 30.3; H, 2.9; N, 3.4. FT-IR (neat): $\nu = 1678(\text{w}), 1605(\text{m}), 1564(\text{w}), 1481(\text{s}), 1442(\text{m}), 1378(\text{s}), 1321(\text{m}), 1230(\text{s}), 1163(\text{w}), 1111(\text{w}), 1032(\text{m}), 928(\text{m}), 852(\text{s}), 733(\text{s}) \text{ cm}^{-1}$.

6–17 catalyzed O-acylative cleavage of cyclic ethers

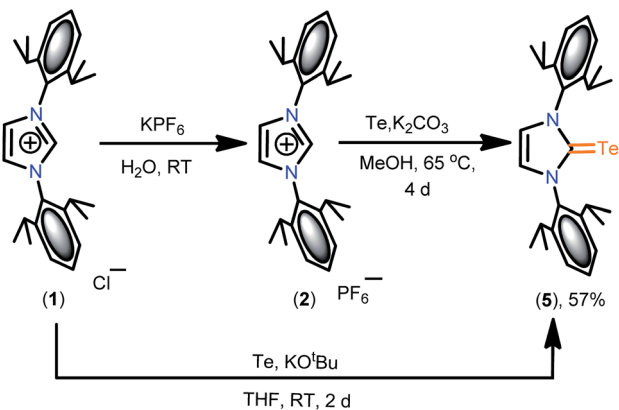
The catalytic reactions were carried out under very mild conditions using acid chlorides (acetyl/benzoyl chloride) in dichloromethane, to which THF/2-MTHF/THP/1,4-dioxane was added after 2–3 minutes then catalyst (**6–17**) was added and allowed to stir at room temperature. The progress of reaction was monitored by TLC. After the completion, water (30 mL) was added to the reaction mixture to afford a suspension, which was extracted by chloroform (3 × 25 mL). Then these combined extracts were dried (Na₂SO₄) and concentrated under *vacuo* to produce an oily liquids. The disappearance of the starting materials and materialization of products were conveniently scrutinized by ¹H NMR spectroscopy.

Results and discussion

Synthesis and characterization of 3–5 and 3–5a

The ligands **3**, **3a**, **4**, **4a** and **5a** were synthesized as reported in the literature.²⁴ Although, **5** was isolated from reaction between Cy₃P(E) and IPr by chalcogen transfer route,²⁵ herein, we report the straight forward route to isolate **5** in good yield, together with a crystal structure. An attempt to synthesize **5** by mixing tellurium powder with **1** in presence of potassium carbonate in methanol was failed. Therefore, IPr·HPF₆ (**2**) was treated with tellurium in the presence of K₂CO₃ to result **5** in fairly good yields. Sequentially, yield of **5** was improved when reaction time was extended from two days to four days. Alternatively, **5** was synthesized in the same yield from the reaction between **2** and potassium *tert*-butoxide at room temperature over a period of two days (Scheme 2).

The light green crystals of **5** were isolated from a saturated solution in a mixture of toluene and *n*-hexane. The formation of



Scheme 2 Synthesis of 5.

5 was confirmed by ^1H and ^{13}C NMR. In ^{13}C NMR, the carbene carbon attached to Te appeared at $\delta = 145.9$ ppm, which is shifted by about $\delta = 20$ ppm upfield compared to the chemical

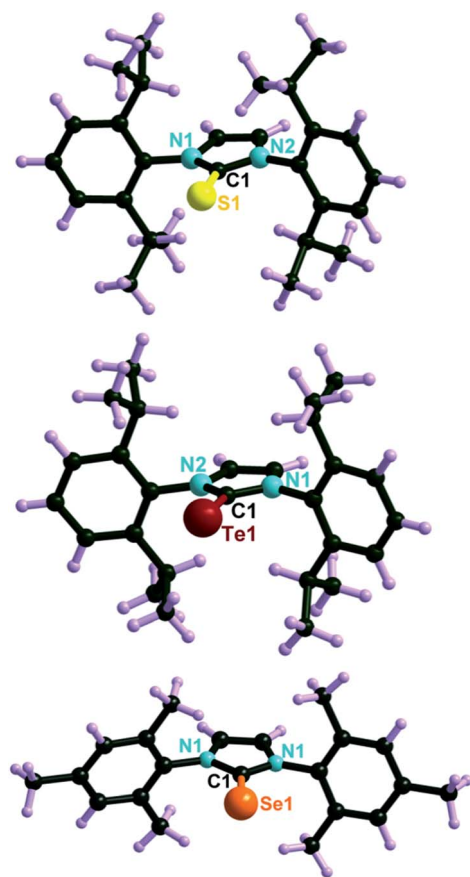


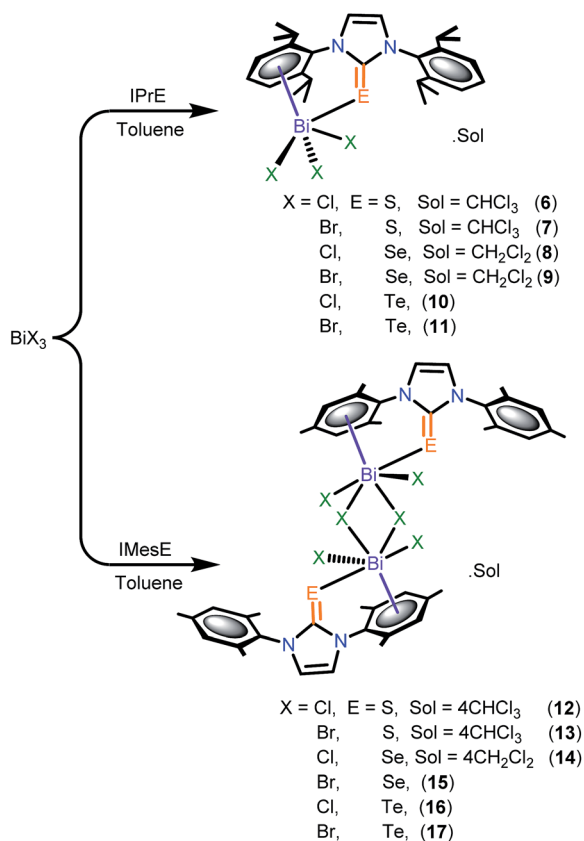
Fig. 1 Top: molecular structures of 3. Selected bond lengths (Å) and angles ($^\circ$) of 3: C(1)–S(1), 1.670(3); C(1)–N(1), 1.371(3); C(1)–N(2), 1.368(3); N(1)–C(1)–N(2), 104.6(2); N(1)–C(1)–S(1), 127.2(2); N(2)–C(1)–S(1), 128.16(19). Middle: molecular structures of 5. Selected bond lengths (Å) and angles ($^\circ$) of 5: C(1)–Te(1), 2.055(3); C(1)–N(1), 1.367(4); C(1)–N(2), 1.356(4); N(1)–C(1)–N(2), 105.0(2); N(1)–C(1)–Te(1), 126.7(2); N(2)–C(1)–Te(1), 128.2(2). Bottom: molecular structures of 4a. Selected bond lengths (Å) and angles ($^\circ$) of 4a: C(1)–Se(1), 1.827(6); C(1)–N(1), 1.365(6); N(1)–C(1)–N(1), 104.8(5); N(1)–C(1)–Se(1), 127.6(3).

shift value of carbene carbon attached to S ($\delta = 167.0$ ppm, 3)²⁷ and Se ($\delta = 162.2$ ppm, 4).²⁶ Moreover, the solid state structures of 3 and 5 were unambiguously confirmed by single crystal X-ray diffraction techniques. The molecules 3 and 5 crystallized in the monoclinic space group $P2_1/n$ (Fig. 1). The selected structural parameters are listed in Table S1a (see ESI†). 4a crystallized in the orthorhombic space group, $Pbcn$ from its saturated solution of dichloromethane layered with *n*-hexane (Fig. 1). The selected bond lengths and angles are listed in Fig. 1. The increase in C=E bond length can be observed from thione to tellone (1.670(3) Å for 3, 1.853(7) Å for 4 (ref. 26) and 2.055(3) Å for 5) due to the increase in size (atomic radii) and weak $\pi\pi$ - $\pi\pi$ interactions in the same order. The C=S bond length in 3 (1.670(3) Å) is almost equal to that of IMes=S (IMes = 1,3-dimesitylimidazole-2-thione) (1.6756(18) Å) and for IAd=S (IAd = 1,3-diadamantylimidazole-2-thione) (1.686(12) Å).²⁷ The C=Te bond length of 5 (2.055(3) Å) is comparable to that of IMes=Te (1,3-dimesitylimidazole-2-tellone) (2.066(3) Å).²⁸ The C=Se bond length (1.827(6) Å) in 4a is almost comparable to that of 4 (1.822(4) Å). The N–C bond lengths and bond angles N–C–N of 3–5a are comparable. The N–C–E bond angles of 3–5a are comparable, which indicates the typical sp^2 hybridization of carbene carbon in chalcogenones.

Synthesis and characterization of 6–17

Subsequently, 3–5a were used as potential ligands to isolate the first discrete monomeric bismuth chalcogenones, [IPrEBiX₃], E = S, X = Cl (6), Br (7); E = Se, X = Cl (8), Br (9); E = Te, X = Cl (10), Br (11) and dimeric bismuth chalcogenones, [IMesEBiX₃], E = S, X = Cl (12), Br (13); E = Se, X = Cl (14), Br (15); E = Te, X = Cl (16), Br (17) (Scheme 3). The compounds 6–17 were synthesized from chalcogenones 3, 3a, 4, 4a, 5 and 5a, respectively, by treating with bismuth halides in toluene. 6–9 and 12–15 were soluble in common organic solvents like CH_2Cl_2 , CHCl_3 , acetone, THF and acetonitrile. The formation of 6–9 and 12–15 was confirmed by elemental analysis, FT-IR, multinuclear (^1H and ^{13}C) NMR, UV-vis and TGA. In ^{13}C NMR, the carbene carbon chemical shift value of 6, 7, 12 and 13 are shifted distinctly upfield ($\delta = 5$ ppm) from those of the corresponding ligands 3 and 3a, respectively, due to a decrease in the pi-acceptance nature of the carbene carbon. In contrast, the carbene carbon chemical shift value of 8, 9, 14 and 15 are nearly comparable with those of the corresponding ligands, 4 and 4a, respectively. The attempts to characterize 10, 11, 16 and 17 by ^1H NMR, ^{13}C NMR and single crystal X-ray techniques were unsuccessful due to the highly dissociative nature of molecules in solution. Thus, the possible solid-state analyses (elemental analysis, FT-IR, UV-vis and TGA) and for 10, 11, 16 and 17 were carried-out and compared with structurally characterized 6–9 and 12–15 (*vide infra*).

Compound 5 reacts immediately with bismuth halides in toluene even at 0 $^\circ\text{C}$. Compound 10 was obtained as oily brick red precipitate, while 11, 16 and 17 were isolated as reddish-brown precipitates. If these reactions were carried out for more than 30 minutes, ill-defined products were obtained as black precipitates. The adducts 10, 11, 16 and 17 were not



Scheme 3 Synthesis of 6–17.

soluble in common organic solvents and underwent decomposition. They were therefore characterized by elemental analysis, FT-IR, solid state UV-vis and TGA techniques.

Single crystal X-ray structure of 6–9 and 12–15

The solid state structures of 6–9 were further confirmed by single crystal X-ray diffraction techniques. 6 (Fig. 2), 8 and 9 crystallized in the monoclinic space group, $P2_1/c$ (Fig. 3). Molecule 7 crystallized in the triclinic space group PT (Fig. 2). Compounds 6 and 7 crystallized with one molecule of CHCl_3 in the lattice, while 8 and 9 crystallized with one molecule of CH_2Cl_2 in the lattice. The crystallographic data for 6–9 are furnished in Table S1a (see ESI[†]) and the important bond parameters are listed in Table S2 (see ESI[†]). The molecular structures of 6–9 are isostructural. 6–9 are the first structurally characterized mononuclear bismuth chalcogen derivatives with a bismuth : chalcogen ratio of 1 : 1.²⁹

The bismuth center in 6–9 is formally tetra coordinated with three halogens and one chalcogenone. As expected for the trivalent group 15 elements, the lone pair electron at the bismuth center occupies at the fifth coordinating site. Similar such pseudo-trigonal bipyramidal $[(E)\text{BiX}_3]$ core geometry is very rare for bismuth chalcogenone complexes. The only example known with similar geometry is the arsenic thione, $[(\text{dmit})\text{AsCl}_3]$ ($\text{dmit} = 1,3\text{-dimethyl-2}(3H)\text{-imidazolethione}$).³⁰ In addition, molecules 6–9 shows $\text{Bi}\cdots\text{aryl}$ π interactions (3.458–3.263 Å in 6; 3.507–3.338 Å in 7; 3.430–3.331 Å in 8; 3.511–

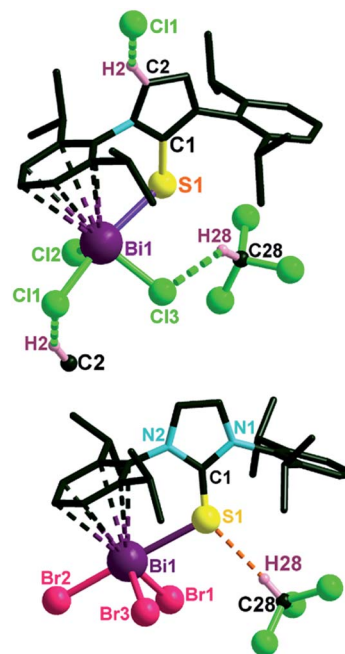


Fig. 2 Top: molecular structure of 6. Non-interacting hydrogen atoms have been omitted for the clarity. Selected bond lengths (Å) and angles (°): C(1)–S(1), 1.696(10), S(1)–Bi(1), 2.929(2), C(1)–S(1)–Bi(1), 108.8(3), N(1)–C(1)–N(2), 106.1(8), N(1)–C(1)–S(1), 130.1(7), N(2)–C(1)–S(1), 123.7(7). D \cdots A distances [Å]: H(2) \cdots Cl(1), 2.871; H(28) \cdots Cl(3), 2.824; C–D \cdots A angles [°]: C(2)–H(2) \cdots Cl(1), 145.32; C(28)–H(28) \cdots Cl(3), 135.06. Bottom: molecular structure of 7. Non-interacting hydrogen atoms and CHCl_3 have been omitted for the clarity. Selected bond lengths (Å) and angles (°): C(1)–S(1), 1.694(7), S(1)–Bi(1), 2.940(18), C(1)–S(1)–Bi(1), 114.1(2), N(1)–C(1)–N(2), 105.9(6), N(1)–C(1)–S(1), 125.5(5), N(2)–C(1)–S(1), 128.7(5). H(28) \cdots S(1) distance is 2.797 Å; C(28)–H(28) \cdots S(1) angles is 175.23°.

3.332 Å in 9), which is within the range of $\text{Bi}\cdots\text{aryl}$ distances reported for $[\text{BiCl}_3\cdot(\text{C}_6\text{H}_6\text{-}_n\text{Me}_n)]$ (3.168(7) to 3.751(8) Å).³¹ The $\text{Bi}\cdots\text{aryl}$ π interactions in mononuclear bismuth compounds are rare.³² The centroid of the C6-ring (3.083 Å in 6; 3.105 Å in 7; 3.080 Å in 8; 3.111 Å in 9) suggests that a half sandwich $[\text{E}\eta\text{-ArBi(E)(X)}_3]$ class of bismuth environment is present in 6–9.³³ Up-on coordination to bismuth, the C=S bond lengths in 6 and 7 are slightly increased from 1.670(3) Å (for 3) to 1.696(10) Å (for 6) and 1.694(7) Å (for 7) due to the strong σ donor nature. Similarly, the C=Se bond length in 8 and 9 also increased from 1.822(4) Å (for 4) to 1.861(5) Å (for 8) and 1.861(8) Å (for 9). The Bi=S bond length in 6 (2.99(2) Å) and 7 (2.940(18) Å) is almost comparable with those of $[\text{BiCl}_3(\text{mnpit})_2]$ ($\text{mnpit} = 1\text{-methyl-3-(1-propyl)-2}(3H)\text{-imidazolethione}$) (2.933(2) Å), $[\text{BiCl}_3(\text{mipit})_2]$ ($\text{mipit} = 1\text{-methyl-3-(2-propyl)-2}(3H)\text{-imidazolethione}$) (2.937(2) Å) and $[\text{BiCl}_3(\text{meimtH})_{2.5}\cdot\text{H}_2\text{O}]$ ($\text{meimtH} = 1\text{-methyl-2}(3H)\text{-imidazolethione}$) (2.948(2) Å).³⁴ The Bi=Se bond lengths in 8 (2.971(5) Å) and 9 (2.980(8) Å) are comparable with that of $[\text{BiCl}_3([\text{8}]\text{aneSe}_2)]$ ($\text{aneSe}_2 = 1,5\text{-diselenacyclooctane}$) (2.988(4) Å to 3.067(4) Å) and $[\text{BiBr}_3([\text{16}]\text{aneSe}_4)]$ ($\text{aneSe}_4 = 1,5,9,13\text{-tetraselenacyclohexadecane}$) (2.952(2) Å to 3.095(2) Å).³⁵

Surprisingly, the molecular packing of 6–9 is not comparable. The possible weak interactions in 6–9 are shown in Fig. 2 and 3. As shown in Fig. 2, the hydrogen bonded polymeric chain

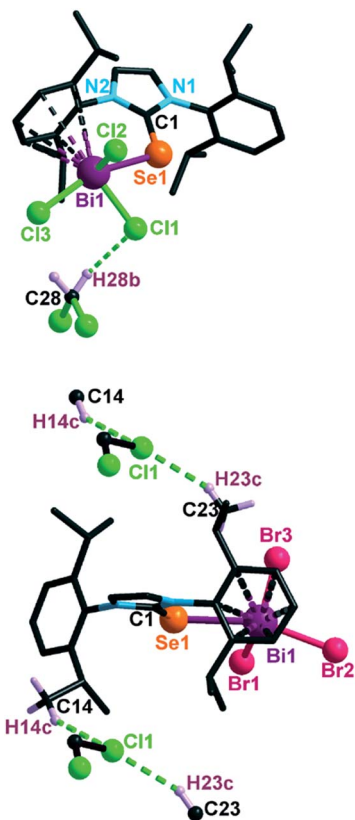


Fig. 3 Top: molecular structure of **8** with C–H...Cl hydrogen bond. Non-interacting hydrogen atoms have been omitted for the clarity. Selected bond lengths (Å) and angles (°): C(1)–Se(1), 1.861(5), Se(1)–Bi(1), 2.971(5), C(1)–Se(1)–Bi(1), 110.94(13), N(1)–C(1)–N(2), 106.1(4), N(1)–C(1)–Se(1), 125.3(3), N(2)–C(1)–Se(1), 108.5(3). D...A distances [Å]: H(28a)...Cl(2), 2.907; H(28b)...Cl(1), 2.682; C–D...A angles [°]: C(28)–H(28a)...Cl(2), 148.09; C(28)–H(28b)...Cl(1), 141.29. Bottom: Molecular structure of **9** with C–H...Cl hydrogen bond. Non-interacting hydrogen atoms have been omitted for the clarity. Selected bond lengths (Å) and angles (°): C(1)–Se(1), 1.861(8), Se(1)–Bi(1), 2.980(8), C(1)–Se(1)–Bi(1), 111.5(2), N(1)–C(1)–N(2), 105.9(6), N(1)–C(1)–Se(1), 129.2(5), N(2)–C(1)–Se(1), 124.8(5). D...A distances [Å]: H(14c)...Cl(1), 2.874; H(23c)...Cl(1), 2.875; C–D...A angles [°]: C(14)–H(14c)...Cl(1), 149.33; C(23)–H(23c)...Cl(1), 144.30.

through C–H...Cl interactions are observed in **6** (also observed from corresponding down field shift of imidazole CH proton at $\delta = 7.21$ ppm), while **7** exist as a monomer with an unusual C(28)–H(28)...S type of hydrogen bond. The H(28)...S distance (2.797 Å) and C(28)–H(28)...S angle (175.23°) shows that the C(28)–H(28)...S hydrogen bonding interaction is relatively stronger than C–H...S hydrogen bonding interaction observed for *N,N'*-dimethylthioformamide (H...S 3.781(7) Å, 175.4(7)°).³⁶ Similarly, **8** exists in the monomeric form with intramolecular hydrogen bonding between CH₂Cl₂ protons and BiCl₃ moiety (Fig. 3). The molecule **9** forms a hydrogen bonded polymeric chain through C–H...Cl interaction (Fig. 3), which is further supported by ¹H NMR where the ¹PrCH protons ($\delta = 1.37$ ppm) are shifted more down field due to hydrogen bonding with a dichloromethane molecule.

The solid state structures of **12–15** were further confirmed by single crystal X-ray diffraction technique. Compounds **12** and **13**

crystallized with one molecule of CHCl₃ in the lattice, while **14** crystallized with one molecule of CH₂Cl₂ in the lattice. The molecule **12** crystallized in monoclinic space group, *P*₂₁/*n* (Fig. 4), while **13** crystallized in the triclinic space group *P* $\bar{1}$ (Fig. 5). The molecules **14** and **15** crystallized in the monoclinic space group, *P*₂₁/*c* (Fig. 6 and 7). The crystallographic data for **4a** and **12–15** are furnished in Table S1b (see ESI†) and the important bond parameters are listed in Table S3 (see ESI†). The molecular structures of **12–15** are isostructural. The molecular structures of **12–15** are the first structurally characterized dimeric bismuth chalcogen derivatives with a 1 : 1 bismuth : -chalcogen mole ratio. The bismuth center in **12–15** is formally penta-coordinated, where two bridged halogens (X(2)), one chalcogenone (E(1)), one terminal halogen (X(1)) and the bismuth center are in the basal plane, while one halogen (X(3)) occupies the apical position. As expected for a penta-coordinated group 15 element in oxidation state (iii), the lone pair at bismuth

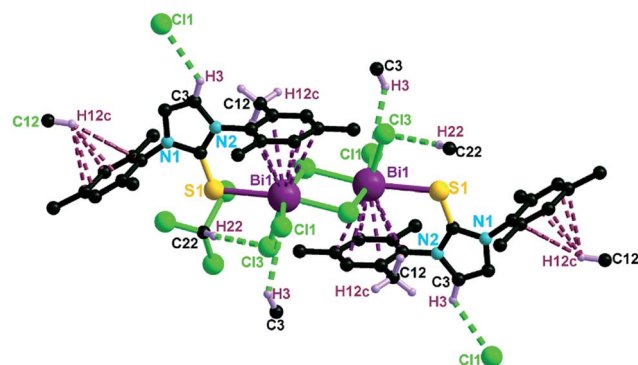


Fig. 4 Molecular structure of **12** with C–H...Cl, C–H... π and Bi... π types of interactions. Non-interacting hydrogen atoms have been omitted for the clarity. Selected bond lengths (Å) and angles (°): C(1)–S(1), 1.683(19), S(1)–Bi(1), 2.874(5), C(1)–S(1)–Bi(1), 112.6(6), N(1)–C(1)–N(2), 104.1(15), N(1)–C(1)–S(1), 131.3(12), N(2)–C(1)–S(1), 124.6(14). D...A distances [Å]: Bi(1)... π (aryl), 3.102; H(12C)... π , 2.858; H(3)...Cl(1), 2.797; H(22)...Cl(3), 2.685; C–D...A angles [°]: C(12)–H(12C)... π , 131.22; C(3)–H(3)...Cl(1), 128.60; C(22)–H(22)...Cl(3), 147.77.

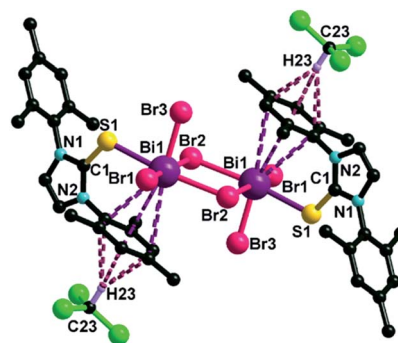


Fig. 5 Molecular structure of **13** with C–H... π and Bi... π types of interactions in **13**. Non-interacting hydrogen atoms have been omitted for the clarity. Selected bond lengths (Å) and angles (°): C(1)–S(1), 1.703(9), S(1)–Bi(1), 2.778(2), C(1)–S(1)–Bi(1), 110.8(3), N(1)–C(1)–N(2), 109.9(7), N(1)–C(1)–S(1), 123.1(6), N(2)–C(1)–S(1), 130.2(6). D...A distances [Å]: Bi(1)... π (aryl), 3.273; H(23)... π , 2.604; C–D...A angles [°]: C(23)–H(23)... π , 169.71.

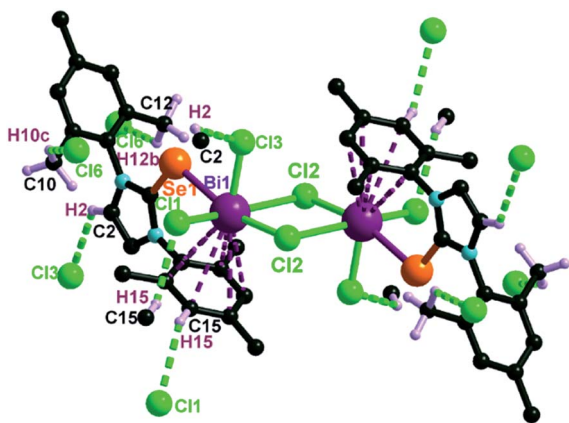


Fig. 6 Molecular structure of **14** with C–H...Cl and Bi... π types of interactions in **14**. Non-interacting hydrogen atoms have been omitted for the clarity. Selected bond lengths (Å) and angles ($^{\circ}$): C(1)–Se(1), 1.870(9), Se(1)–Bi(1), 2.8931(10), C(1)–Se(1)–Bi(1), 109.8(3), N(1)–C(1)–N(2), 106.3(7), N(1)–C(1)–Se(1), 129.0(7), N(2)–C(1)–Se(1), 124.7(7). D...A distances [Å]: Bi(1)... π (aryl), 3.151; H(2)...Cl(3), 2.816; H(10c)...Cl(6), 2.649; H(15)...Cl(1), 2.865; C–D...A angles [$^{\circ}$]: C(2)–H(2)...Cl(3), 124.20; C(15)–H(15)...Cl(1), 137.05; C(10)–H(10C)...Cl(6), 143.77.

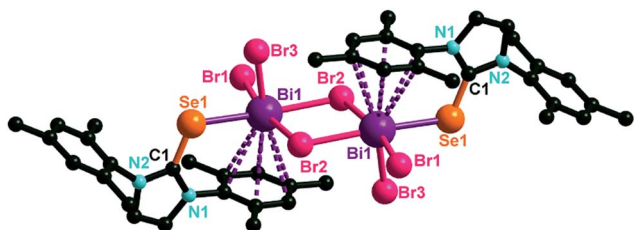


Fig. 7 Molecular structure of **15**. Hydrogen atoms have been omitted for the clarity. Selected bond lengths (Å) and angles ($^{\circ}$): C(1)–Se(1), 1.866(6), Se(1)–Bi(1), 2.9251(7), C(1)–Se(1)–Bi(1), 108.54(19), N(1)–C(1)–N(2), 105.9(5), N(1)–C(1)–Se(1), 129.6(4), N(2)–C(1)–Se(1), 124.5(4). Bi(1)... π (aryl) distance 3.149 Å. (IV) Molecular packing of **15**. View along *b* axis. Bi(1)... π (aryl) interaction is not shown.

occupies the sixth coordinating site. The geometry of the bismuth center in **12–15** is comparable with [2,6-Mes₂-4-R-C₆H₂BiX₂]₂ (R = ^tBu or H).³⁷ Such square-pyramidal [(E)BiX₄] core geometry is rare for bismuth chalcogenones. The C=S bond lengths (1.683(19) Å for **12**; 1.703(9) Å for **13**) and C=Se bond lengths (1.870(9) Å for **14**; 1.866(6) Å for **15**) are increased compared to **3a** (1.675(18) Å)²⁷ and **4a** (1.827(6) Å), respectively.

Molecule **12** shows a short Bi(1)... π (aryl) interaction (3.102 Å) compared to **13** (3.273 Å), **14** (3.151 Å) and **15** (3.149 Å). Although molecules **12–15** show a similar geometry, they deviate through hydrogen bonding. Possible weak interactions in **12–15** are shown in Fig. 4–7. Interestingly, molecules **12** and **14** show a C–H...Cl type of hydrogen bonding, in contrast, this is absent in **13** and **15**. Surprisingly, molecules **12** and **13** show a rare C–H... π (aryl) interaction. In **12**, a C–H... π (aryl) is observed between one of methyl protons, H(12C) and the aryl ring. Such an interaction in **13** is found between CHCl₃ and one of the aryl rings. The C–H... π (aryl) interaction in **13** (H(23)... π , 2.604 Å; C(23)–H(23)... π , 169.71 $^{\circ}$) much stronger than **12** (H(12C)... π , 2.858 Å;

C(12)–H(12C)... π , 131.22 degrees), however, the observed C–H... π (aryl) interaction is relatively strong.³⁸ The (Me)H(12C)... π (aryl) interactions in **12** and (Me)H(10C/12B)...Cl(6) interactions in **14** are clearly noticeable in the corresponding ¹H NMR chemical shift value (δ = 2.17 ppm, slightly shifted downfield). The aromatic protons in ¹H NMR spectrum of **14** are highly deshielded (δ = 7.16 ppm) due to H(15)...Cl(1) interactions. The Bi=E bond lengths in **12–15** are slightly shorter than **6–9** due to the dimeric form.

UV-visible absorption study

UV-visible absorption spectra of **3–5** were measured in dichloromethane at room temperature, and displayed a bathochromic shift from **3** (233 and 271 nm), **4** (238 and 293 nm) to **5** (240, 323 and 365 nm) (see ESI[†]). In the solid state UV-vis spectra of **3–5** are nearly comparable with solution state absorption spectra (221 and 267 nm for **3**; 241 and 295 nm for **4**; 221, 302 and 356 nm for **5**) (see ESI[†]). Thus, the molecular association and stability of **3–5** are comparable. The additional absorption observed for **5** at 365 nm (solution state) and 356 (solid state) nm can be attributed to the imidazole to tellurium charge transfer.

The solid state UV-vis spectra of **3–5a** are not comparable with solution state absorption spectra (258 and 381 nm for **3a**; 271 and 386 nm for **4a**; 221, 338 and 465 nm for **5a**) (see ESI[†]). Thus, the molecular association and stability of **3–5a** are not comparable in both the states. The additional absorption observed for **5a** at 355 nm (solution state) and 465 (solid state) nm can be attributed to the imidazole to tellurium charge transfer.

As shown in Fig. 8(I), the absorption strength of **6** decreases compared to **3**, while it increases for **7**. In solid state, the absorption nature of **6** and **7** decreases compared to **3**. (Fig. 8(II)). Interestingly, the solution state absorption intensity of **8** and **9** are lower than **4** (Fig. 8(III)), while in the solid state the reverse trend is observed (Fig. 8(IV)). Furthermore, in the solid state UV-vis spectra of **5**, **10** and **11** are shown in Fig. 8(V), where the absorption strength of **10** and **11** are slightly higher than **5**. As shown in Fig. 9(I), the absorption strength of **12** and **13** decreases compared to **3a**. In solid state, the absorption nature of **12** decreases and **13** is almost comparable with **3a**. (Fig. 9(II)). Interestingly, the solution state absorption intensity of π - π^* (high) and n - π^* (low) in **14** and **15** are inverse to that of **4a** (Fig. 9(III)). In the solid state, **14** and **15** shows high absorption (Fig. 9(IV)). Furthermore, the solid state UV-vis spectra of **5a**, **16** and **17** are shown in Fig. 9(V), where the absorption strength of **16** and **17** is higher than that of **5a**.

TGA analysis

In order to understand the thermal decomposition pathway of **3–17**, thermogravimetric analysis (TGA) (10 $^{\circ}$ C min⁻¹, 30–1000 $^{\circ}$ C, under N₂ atmosphere) was carried out on **3–17** (Fig. 10). **3**, **3a**, **4** and **4a** show enough stability up to 300 $^{\circ}$ C, and show sudden weight loss in single step but **5** lost weight in two steps and **5a** in three steps, which can be attributed to the decomposition of organic moieties.

The TGA profiles of **6–17** are distinctly different from that of the corresponding chalcogenones. The residual weights

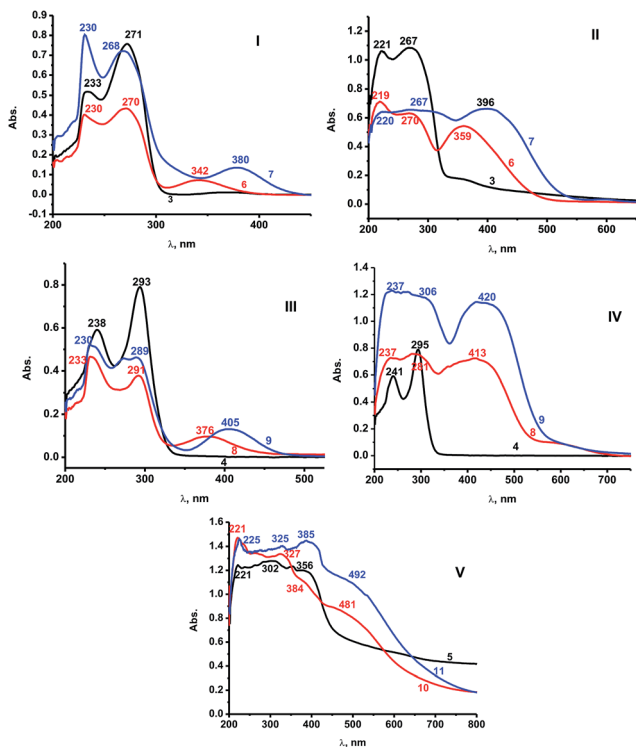


Fig. 8 (I) Solution state UV-vis spectra of **3**, **6** and **7** in DCM at 25 °C (3.8×10^{-2} M); (II) solid state UV-vis spectra of **3**, **6** and **7**; (III) solution state UV-vis spectra of **4**, **8** and **9** in DCM at 25 °C (3.8×10^{-2} M); (IV) solid state UV-vis spectra of **4**, **8** and **9**; (V) solid state UV-vis spectra of **5**, **10** and **11**.

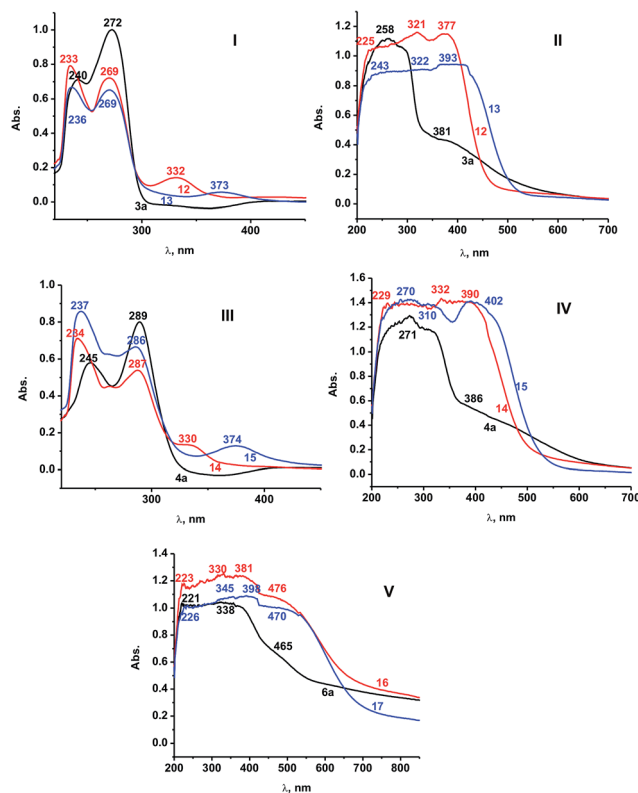


Fig. 9 (I) Solution state UV-vis spectra of **3a**, **12** and **13** in DCM at 25 °C (3.8×10^{-2} M); (II) solid state UV-vis spectra of **3a**, **12** and **13**; (III) solution state UV-vis spectra of **4a**, **14** and **15** in DCM at 25 °C (3.8×10^{-2} M); (IV) solid state UV-vis spectra of **4a**, **14** and **15**; (V) solid state UV-vis spectra of **5a**, **16** and **17**.

obtained from the TGA profiles of **13** and **15** (3% for **13** and 13% for **15**) are not in agreement with the calculated values for Bi_2E_3 , which is unclear at this stage. Compounds **6**, **10**, **12**, **14** and **16** left with the calculated amount of residue.

Bismuth(III) catalyzed *O*-acylative cleavage of cyclic ethers

The selective *O*-acylative cleavage and successive intramolecular trapping of cations generated from cyclic ethers using bismuth(III) halides as catalyst shows much potential in organic synthesis. Despite the popularity and versatility of metal mediated C–O bond cleavages of cyclic ethers like THF/2-MTHF/THP to deliver 4-haloalkyl alkanooates, there are very few examples of bismuth mediated C–O bond cleavage reactions known in the literature.^{43,44} Herein, we have demonstrated a mild and regioselective catalytic applications for the acylative cleavage of cyclic ethers using **6–17** as catalysts (Scheme 4). Initially, the reaction between THF and acetyl chloride was investigated in the presence of **6–17** under mild conditions. The reaction progress was continually monitored using TLC (Table 1). After completion of the reaction, the routine workup gave 4-chlorobutylacetate in excellent yield (Table 1, entries 1–12, Yield 80–98%). During our investigations THF reacts with both acetylchloride in 15–24 h with maximum conversion of starting materials. To understand the role of well-defined, discrete catalysts, the reaction between THF and acetyl chloride was investigated in the presence of *in situ* generated catalyst **6** by

mixing IPRs (**3**) and BiCl_3 (Table 1, Entry 13). As evidenced, the *in situ* generated catalyst is not as efficient as compared to **6** (although the starting material conversion is 98% in 30 h, the yield (86%) is not quite as good as for other examples. Besides, as shown in entries 14 and 15, the catalytic performance of BiX_3 , X = Cl and Br is comparable with entry 13. Thus, the discrete catalysts **6–17** are more efficient than the *in situ* generated complexes or BiX_3 . As expected, the catalytic efficiency of **6–17** can be attributed to their solubility and electronic nature. Among entries 1–15, catalyst **6** depicted 100% conversion (Table 1, Entry 1) in the least time with excellent yield (Table 1, Entry 1, 15 h), while catalyst **16** showed less starting material conversion (88%) and lower yield (80%) in 24 h (Table 1, Entry 11).

Subsequently, we extended the acylative cleavage of 2-methyl tetrahydrofuran with acid chloride in the presence of **6–17** in DCM at room temperature for 2 h (Scheme 5 and Table SS4 in ESI†). As shown in Fig. 11, catalyst **6** seems to be the most efficient catalyst to produce 4-chloropentylacetate in excellent yield (98%) within 2 h.

Encouraged by our initial results, we sought to examine the scope and the generality of the method under the optimized reaction conditions. Thus, a variety of cyclic ethers like 2-methyl THF, tetrahydropyran (THP) and 1,4-dioxane have been

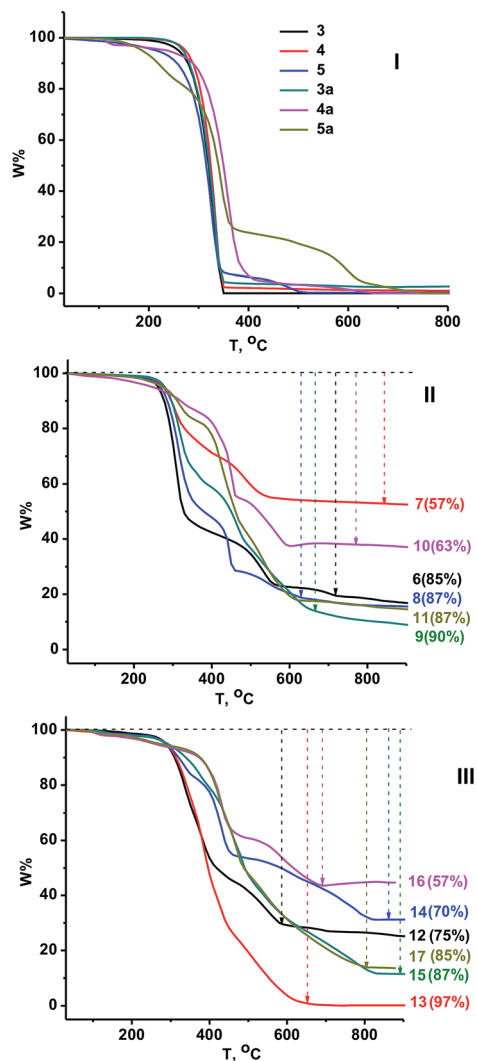
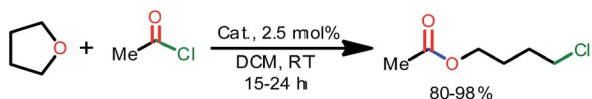


Fig. 10 Top: TGA profiles of 3–5a; Middle: TGA curves of 6–11. Bottom: TGA profiles of 12–17. 10 °C min⁻¹ under N₂ atmosphere.

investigated with acetyl and benzoyl chloride in the presence of catalyst **6** (Table S5 in ESI[†]). 2-Methyl-THF yields regioselective product with 100% conversion when treated with acetyl and benzoyl chloride in the presence of **6** within 2–4 h (Table S5,† entries 2 and 3). Although, the reaction between THF and benzoyl chloride mediated by **6** is efficient (Table S5,† entries 1), the catalytic conversion is very slow compared to entries 2 and 3 (Table S5[†]). In contrast, **6** is not very efficient for the catalytic conversion of tetrahydropyran (THP) or 1,4-dioxane as shown in entries 4–7 (Table S5[†]). Treatment of THP with acetyl chloride in the presence of **6** gave 5-chloropentylacetate in 30% yield, while benzoyl chloride afforded the corresponding 5-chloropentyl

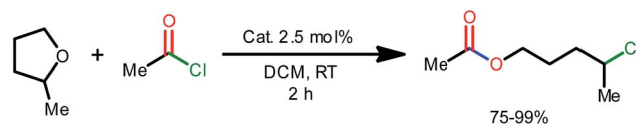


Scheme 4 4-Chlorobutylacetate from O-acylative cleavage of tetrahydrofuran.

Table 1 4-Chlorobutylacetate from O-acylative cleavage of tetrahydrofuran^a

E	Cat.	T (h)	SMC ^b (%)	Y (%)
1	6	15	100	98
2	7	16	98	96
3	8	16.5	95	90
4	9	16	93	90
5	10	18	90	85
6	11	18	89	82
7	12	20	92	90
8	13	18	91	86
9	14	20	93	90
10	15	20	92	88
11	16	24	88	80
12	17	24	89	82
13	3 and BiCl ₃	30	98	86
14	BiCl ₃	30	93	85
15	BiBr ₃	30	88	80

^a E – entry; SM – starting materials; SMC – starting materials conversion; T – time, Y – yield. ^b % yields were calculated based on the weight along with its conversion.



Scheme 5 4-Chloropentylacetate from acylative cleavage of 2-methyl tetrahydrofuran.

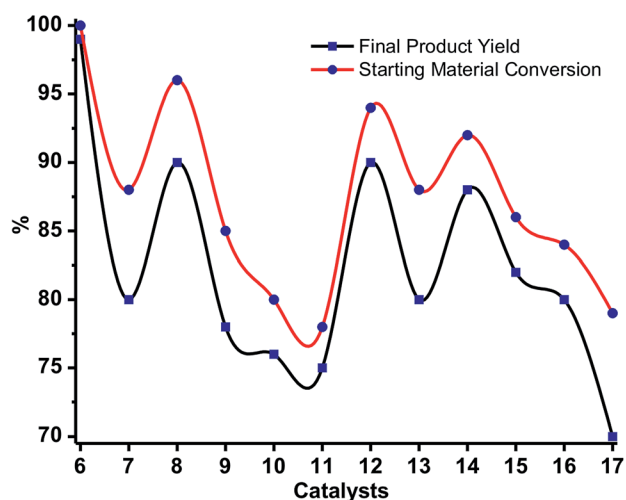


Fig. 11 4-Chloropentylacetate from acylative cleavage of 2-methyl tetrahydrofuran at room temperature in 2 h.

benzoate in 20% yield after 48 h. Notably, **6** is not efficient enough to activate a cyclic polyether such as 1,4-dioxane; as shown in entries 6 and 7 in Table S5; † the yield is not appreciable even after 48 h and there was no further improvement by extending the time up to 4 days. The greater strain within five-membered THF compared to six-membered THP is evident in the extent to which the latter undergoes acylative cleavage with

slow reaction rates. In contrast to the earlier works, our work does not require any extra solvent and elevated temperatures.

Conclusions

In summary, the first mononuclear bismuth heavier chalcogen derivatives **6–11** and binuclear bismuth heavier chalcogen derivatives **12–17** were isolated with bismuth and heavier chalcogen ratio of 1 : 1.‡ Molecules **6–17** were isolated with rare structural features. This work therefore offers an important structural example of $\pi \cdots \text{Bi}$, $\pi \cdots \text{H-C}$ and $\text{S} \cdots \text{H-C}$ interactions along with the precise nature of $\text{E} \cdots \text{Bi}$ ($\text{E} = \text{S}, \text{Se}$ and Te) bonding. The catalytic properties of the complexes were tested in the *O*-acylative cleavage of cyclic ethers. The catalytic activities provided by the metal complexes follow an almost similar trend, in which (i) the mononuclear complex **6** displays the best efficiencies, (ii) the thione–bismuth complexes are more active than selone and tellone analogues, and (iii) all complexes having a 2,6-diisopropylphenyl tag display better activities than the related complexes with a mesityl group. We believe that the catalytic results shown by these complexes may be explained by considering the possibility that the chalcogenone ligands in the metal complexes play a role in the overall catalytic reaction, mainly due to their σ donating capabilities. In the case of the better catalytic activities provided by the mononuclear complex **6**, in comparison to **7–17**, we tentatively propose that the shorter S–Bi distance along with coordinately unsaturated bismuth(III) center increases its catalytic activity in comparison to the situation shown by **7–17**. The asymmetric version of the synthesis is currently underway in our laboratories and this will subsequently be expanded to other synergic ligands.

Acknowledgements

We gratefully acknowledge the DST-SERB (SB/S1/IC-07/2014) for financial support. KS thank UGC for the fellowship.

Notes and references

- 1 *Hard and Soft Acids and Bases*, ed. R. G. Pearson, Dowden, Hutchinson & Ross, Stroudsburg, PA, 1973.
- 2 Selected example for simultaneous cancer imaging and therapy: J. Li, F. Jiang, B. Yang, X.-R. Song, Y. Liu, H.-H. Yang, D.-R. Cao, W.-R. Shi and G.-N. Chen, *Sci. Rep.*, 2013, **3**, 1998, 1–7 and references therein.
- 3 Selected examples for thermoelectric material application: (a) Y. S. Hor, A. Richardella, P. Roushan, Y. Xia, J. G. Checkelsky, A. Yazdani, M. Z. Hasan, N. P. Ong and R. Cava, *Phys. Rev. B: Condens. Matter Mater. Phys.*, 2009, **79**, 195208; (b) Y. L. Chen, J. G. Analytis, J.-H. Chu, Z. K. Liu, S.-K. Mo, X. L. Qi, H. J. Zhang, D. H. Lu, X. Dai, Z. Fang, S. C. Zhang, I. R. Fisher, Z. Hussain and Z.-X. Shen, *Science*, 2009, **325**, 178–181; (c) W. Wang, J. Goebel, L. He, S. Aloni, Y. Hu, L. Zhen and Y. Yin, *J. Am. Chem. Soc.*, 2010, **132**, 17316–17324.
- 4 Selected example for optical application: A. D. LaForge, A. Frenzel, B. C. Pursley, T. Lin, X. Liu, J. Shi and D. N. Basov, *Phys. Rev. B: Condens. Matter Mater. Phys.*, 2010, **81**, 125120.
- 5 Selected example for photoelectric application: Y. Yu, W. T. Sun, Z. D. Hu, Q. Chen and L. M. Peng, *Mater. Chem. Phys.*, 2010, **124**, 865–869.
- 6 Selected example for photocatalytic application: T. Wu, X. Zhou, H. Zhang and X. Zhong, *Nano Res.*, 2010, **3**, 379–386.
- 7 (a) M. Imran, B. Neumann, H.-G. Stammer, U. Monkowius, M. Ertl and N. W. Mitzel, *Dalton Trans.*, 2013, **42**, 15785–15795; (b) M. Imran, B. Neumann, H.-G. Stammer, U. Monkowius, M. Ertl and N. W. Mitzel, *Dalton Trans.*, 2014, **43**, 1267–1278; (c) M. D. Spicer and J. Reglinski, *Eur. J. Inorg. Chem.*, 2009, 1553–1574.
- 8 E. S. Raper, *Coord. Chem. Rev.*, 1996, **153**, 199–255.
- 9 E. S. Raper, *Coord. Chem. Rev.*, 1997, 475–564.
- 10 G. Parkin, *New J. Chem.*, 2007, **31**, 1996–2014.
- 11 C. Pattinari, *Scorpionates II: Chelating Borate Ligands*, Imperial College Press, London, 2008, pp. 381–415.
- 12 P. D. Akrivos, *Coord. Chem. Rev.*, 2001, **213**, 181–210.
- 13 For selected examples: (a) M. Arca, T. Aroz, M. C. Gimeno, M. Kulcsar, A. Laguna, T. Lasanta, V. Lippolis, J. M. López-de-Luzuriaga, M. Monge and M. E. Olmos, *Eur. J. Inorg. Chem.*, 2011, 2288–2297; (b) D. J. Williams, A. Shilatifard, D. VanDerveer, L. A. Lipscomb and R. L. Jones, *Inorg. Chim. Acta*, 1992, **202**, 53–57; (c) F. Bigoli, P. Deplano, F. A. Devillanova, V. Lippolis, M. L. Mercuri, M. A. Pellinghelli and E. F. Trogu, *Inorg. Chim. Acta*, 1998, **267**, 115–121.
- 14 L. P. Battaglia, A. B. Corradi, M. Nardelli and M. E. V. Tani, *J. Chem. Soc., Dalton Trans.*, 1978, 583–587.
- 15 M. Shu, J. Cui and J. Sun, *Appl. Organomet. Chem.*, 2005, **19**, 184–185.
- 16 P. J. Bailey, M. Lanfranchi, L. Marchiò and S. Parsons, *Inorg. Chem.*, 2001, **40**, 5030–5035.
- 17 M. Lanfranchi, L. Marchiò, C. Mora and M. A. Pellinghelli, *Inorg. Chim. Acta*, 2004, **357**, 367–375.
- 18 M. Careri, L. Elviri, M. Lanfranchi, L. Marchiò, C. Mora and M. A. Pellinghelli, *Inorg. Chem.*, 2003, **42**, 2109–2114.
- 19 J. Reglinski, M. D. Spicer, M. Garner and A. R. Kennedy, *J. Am. Chem. Soc.*, 1999, **121**, 2317–2318.
- 20 D. J. Williams, D. VanDerveer, R. L. Jones and D. S. Menaldino, *Inorg. Chim. Acta*, 1989, **165**, 173–178.
- 21 D. J. Williams, J. T. Anderton, E. A. Armstrong, M. H. Bowen, R. E. Hart, S. K. Tata, D. R. Smith, K. M. White and D. Vanderveer, *Main Group Chem.*, 2007, **6**, 263–270.
- 22 L. P. Battaglia and A. B. Corradi, *J. Chem. Soc., Dalton Trans.*, 1983, 2425–2428.
- 23 S. T. Manjare, S. Yadav, H. B. Singh and R. J. Butcher, *Eur. J. Inorg. Chem.*, 2013, 5344–5357.
- 24 S. Wei, X. G. Wei, X. Su, J. You and Y. Ren, *Chem.–Eur. J.*, 2011, **17**, 5965–5971.

‡ In this paper a word “chalcogenones or heavier chalcogens” represents the molecule with “S, Se and Te”. Therefore “O” (*i.e.* molecules with C=O–Bi bond) should not be considered for the current discussion.

- 25 J. E. McDonough, A. Mendiratta, J. J. Curley, G. C. Fortman, S. Fantasia, C. C. Cummins, E. V. R. Akimova, S. P. Nolan and C. D. Hoff, *Inorg. Chem.*, 2008, **47**, 2133–2141.
- 26 (a) D. J. Nelson, A. Collado, S. Manzini, S. Meiries, A. M. Z. Slawin, D. B. Cordes and S. P. Nolan, *Organometallics*, 2014, **33**, 2048–2058; (b) D. J. Nelson, F. Nahra, S. R. Patrick, D. B. Cordes, A. M. Z. Slawin and S. P. Nolan, *Organometallics*, 2014, **33**, 3640–3645; (c) A. Liske, K. Verlinden, H. Buhl, K. Schaper and C. Ganter, *Organometallics*, 2013, **32**, 5269–5272.
- 27 (a) J. Huang, H. J. Schanz, E. D. Stevens and S. P. Nolan, *Inorg. Chem.*, 2000, **39**, 1042–1045; (b) M. Tretiakov, Y. G. Shermolovich, A. P. Singh, P. P. Samuel, H. W. Roesky, B. Niepötter, A. Visschera and D. Stalke, *Dalton Trans.*, 2013, **42**, 12940–12946.
- 28 A. J. Arduengo III, F. Davidson, H. V. R. Dias, J. R. Goerlich, D. Khasnis, W. J. Marshall and T. K. Prakasha, *J. Am. Chem. Soc.*, 1997, **119**, 12742–12749.
- 29 (a) W. Levason, S. D. Orchard and G. Reid, *Coord. Chem. Rev.*, 2002, **225**, 159–199; (b) S. Traut, A. P. Hähnel and C. V. Hänisch, *Dalton Trans.*, 2011, **40**, 1365–1371; (c) T. Sasamori, E. Mieda, N. Takeda and N. Tokitoh, *Angew. Chem., Int. Ed.*, 2005, **44**, 3717–3720; (d) S. Heimann, D. Bläser, C. Wölper and S. Schulz, *Organometallics*, 2014, **33**, 2295–2300.
- 30 (a) D. J. Williams, C. O. Quicksall and K. J. Wynne, *Inorg. Chem.*, 1978, **17**, 2071–2073; (b) D. J. Williams and K. J. Wynne, *Inorg. Chem.*, 1978, **17**, 1108–1115; (c) D. J. Williams and A. Viehbeck, *Inorg. Chem.*, 1979, **18**, 1823–1825.
- 31 (a) W. Frank, J. Schneider and S. J. Müller-Becker, *J. Chem. Soc., Chem. Commun.*, 1993, 799–800; (b) W. Frank and V. Reiland, *Acta Crystallogr.*, 1998, **C54**, 1626–1628; (c) H. Schmidbaur, J. M. Wallis, R. Nowak, B. Huber and G. B. Müller, *Ber. Bunsen-Ges.*, 1987, **120**, 1837–1843; (d) A. Schier, J. M. Wallis, G. Müller and H. Schmidbaur, *Angew. Chem., Int. Ed. Engl.*, 1986, **25**, 757–759; (e) S. M. Becker, W. Frank and J. Schneider, *Z. Anorg. Allg. Chem.*, 1993, **619**, 1073–1082; (f) H. Schmidbaur, R. Nowak, A. Schier, J. M. Wallis, B. Huber and G. B. Müller, *Ber. Bunsen-Ges.*, 1987, **120**, 1829–1835.
- 32 I. Caracelli, I. Haiduc, J. Z. Schpector and E. R. T. Tiekink, *Coord. Chem. Rev.*, 2013, **257**, 2863–2879 and references there in.
- 33 K. Y. Monakhov, C. Gourlaouen, T. Zessin and G. Linti, *Inorg. Chem.*, 2013, **52**, 6782–6784.
- 34 (a) D. J. Williams, A. M. Hutchings, N. E. McConnell, R. A. Faucher, B. E. Huck, C. A. S. Brevett and D. VanDerveer, *Inorg. Chim. Acta*, 2006, **359**, 2252–2255; (b) D. J. Williams, J. T. Anderton, E. A. Armstrong, M. H. Bowen, R. E. Hart, S. K. Tata, D. R. Smith, K. M. White and D. Vanderveer, *Main Group Chem.*, 2007, **6**, 263–270.
- 35 A. J. Barton, A. R. J. Genge, W. Levason and G. Reid, *Dalton Trans.*, 2000, 2163–2166.
- 36 H. Borrmann, I. Persson, M. Sandström and C. M. V. Stålhandske, *J. Chem. Soc., Perkin Trans. 1*, 2000, 393–402.
- 37 H. J. Breunig, N. Haddad, E. Lork, M. Mehring, C. Mügge, C. Nolde, C. I. Raş and M. Schürmann, *Organometallics*, 2009, **28**, 1202–1211.
- 38 (a) M. Nishio, M. Hirota and Y. Umezawa, *The CH/π Interaction. Evidence, Nature, and Consequences*, Wiley-VCH, New York, 1998, p. 15; (b) A. Fujii, K. Shibasaki, T. Kazama, R. Itaya, N. Mikami and S. Tsuzuki, *Phys. Chem. Chem. Phys.*, 2008, **10**, 2836–2843; (c) T. Steiner, *Angew. Chem., Int. Ed.*, 2002, **41**, 48–76; (d) M. Nishio, *CrystEngComm*, 2004, **6**, 130–158.
- 39 D. D. Perrin and W. L. F. Armarego, *Purification of laboratory chemicals*, Pergamon Press, London, 3rd edn, 1988.
- 40 L. Jafarpour, E. D. Stevens and S. P. Nolan, *J. Organomet. Chem.*, 2000, **606**, 49–54.
- 41 O. V. Dolomanov, L. J. Bourhis, R. J. Gildea, J. A. K. Howard and H. Puschmann, *J. Appl. Crystallogr.*, 2009, **42**, 339–341.
- 42 (a) G. M. Sheldrick, *Acta Crystallogr., Sect. A: Found. Crystallogr.*, 1990, **46**, 467–473; (b) G. M. Sheldrick, *SHELXL-97, Program for Crystal Structure Refinement*, Universität Göttingen, Göttingen, 1997.
- 43 (a) W. F. John, G. P. Wyatt and D. Westmoreland, *J. Org. Chem.*, 1983, **48**, 751–753; (b) H. Alper and C.-C. Huang, *J. Org. Chem.*, 1973, **38**(1), 64–71; (c) Q. Guo, T. Miyaji, R. Hara, B. Shen and T. Takahashi, *Tetrahedron*, 2002, **58**, 7327–7334; (d) J. Iqbal and R. R. Srivastava, *Tetrahedron*, 1991, **47**, 3155–3170; (e) S. U. Kulkarni and V. D. Patil, *Heterocycles*, 1982, **18**, 163–167; (f) A. Oku, T. Harada and K. Kita, *Tetrahedron Lett.*, 1982, **23**, 681–684; (g) S. S. Morrell, *Chem. Abstr.*, 1947, **41**, 7411; (h) P. Minceco, C. Saluzzo and R. Ammouroux, *Tetrahedron Lett.*, 1994, **35**, 1553–1556; (i) S. Bhar and B. C. Ranu, *J. Org. Chem.*, 1995, **60**, 745–747; (j) F. Frejje, G. Schat, R. Mierop, C. Blomberg and F. Bickelhaupt, *Heterocycles*, 1977, **7**, 237–240.
- 44 J. M. Bothwell, S. W. Krabbe and R. S. Mohan, *Chem. Soc. Rev.*, 2011, **40**, 4649–4707.